

RESEARCH ARTICLE

10.1002/2016JD025724

Bias correction and downscaling of future RCM precipitation projections using a MOS-Analog technique

Key Points:

- We assess the analog-based Model Output Statistics (MOS) downscaling method for climate change studies
- The MOS-Analog downscaling method is a spatially consistent alternative to standard bias correction methods
- The downscaled results broadly preserve the original RCM climate change signal, except for extreme precipitation indices

Supporting Information:

- Supporting Information S1

Correspondence to:

M. Turco,
turco.mrc@gmail.com

Citation:

Turco, M., M. C. Llasat, S. Herrera, and J. M. Gutiérrez (2017), Bias correction and downscaling of future RCM precipitation projections using a MOS-Analog technique, *J. Geophys. Res. Atmos.*, 122, 2631–2648, doi:10.1002/2016JD025724.

Received 30 JUL 2016

Accepted 1 FEB 2017

Accepted article online 22 FEB 2017

Published online 6 MAR 2017

M. Turco^{1,2} , M. C. Llasat¹ , S. Herrera³ , and J. M. Gutiérrez⁴ 

¹Department of Applied Physics, University of Barcelona (UB), Barcelona, Spain, ²Barcelona Supercomputing Center (BSC), Barcelona, Spain, ³Meteorology Group, Department of Applied Mathematics and Computer Science, Universidad de Cantabria, Santander, Spain, ⁴Meteorology Group, Instituto de Física de Cantabria, CSIC-Universidad de Cantabria, Santander, Spain

Abstract In this study we assess the suitability of a recently introduced analog-based Model Output Statistics (MOS) downscaling method (referred to as MOS-Analog) for climate change studies and compare the results with a quantile mapping bias correction method. To this aim, we focus on Spain and consider daily precipitation output from an ensemble of Regional Climate Models provided by the ENSEMBLES project. The reanalysis-driven Regional Climate Model (RCM) data provide the historical data (with day-to-day correspondence with observations induced by the forcing boundary conditions) to conduct the analog search of the control (20C3M) and future (A1B) global climate model (GCM)-driven RCM values. First, we show that the MOS-Analog method outperforms the raw RCM output in the control 20C3M scenario (period 1971–2000) for all considered regions and precipitation indices, although for the worst-performing models the method is less effective. Second, we show that the MOS-Analog method broadly preserves the original RCM climate change signal for different future periods (2011–2040, 2041–2070, 2071–2100), except for those indices related to extreme precipitation. This could be explained by the limitation of the analog method to extrapolate unobserved precipitation records. These results suggest that the MOS-Analog is a spatially consistent alternative to standard bias correction methods, although the limitation for extreme values should be taken with caution in cases where this aspect is relevant for the problem.

1. Introduction

Precipitation is a challenging variable which is crucial in several sectors, such as agriculture [see, e.g., Ceglar *et al.*, 2016] and hydrology [see, e.g., Llasat *et al.*, 2016], particularly in the context of climate change and/or in applications involving extreme events [Foley, 2010; Rummukainen, 2010]. The coarse resolution (generally few hundred kilometers) and the systematic biases of global climate models (GCMs) prevents the direct application of global climate projections at a regional scale (generally few kilometers) for impact studies. Therefore, dynamical and/or statistical downscaling techniques are typically applied to bridge this gap in order to obtain plausible regional climate change projections of precipitation [see Fowler *et al.*, 2007; Maraun *et al.*, 2010, and references therein]. During the last decade, downscaling has become a strategic topic in national and international climate programs (see, e.g., the World Climate Research Program-endorsed Coordinated Regional Climate Downscaling Experiment (CORDEX) initiative, Giorgi *et al.* [2009], or the European Union (EU)-funded COST Action VALUE, Maraun *et al.* [2015]).

The dynamical downscaling approach is based on regional climate models (RCMs)—with typical resolutions of tens of kilometers—running over limited geographical domains with boundary conditions given by the GCM to be downscaled [Giorgi and Mearns, 1991]. These RCMs explicitly solve mesoscale atmospheric processes and provide spatially and physically consistent outputs. However, they still have considerable biases [Christensen *et al.*, 2008; Herrera *et al.*, 2010; Turco *et al.*, 2013] which are typically adjusted in practical applications using a variety of Model Output Statistics (MOS) methods. Formally, in the MOS downscaling approach, the target variable (e.g., precipitation) simulated by the RCM is directly corrected against the available local-scale observations using appropriate statistical techniques [Marzban *et al.*, 2006; Maraun *et al.*, 2010; Ruiz-Ramos *et al.*, 2016].

The most popular MOS techniques for climate change studies are distribution-wise; that is, the correction function is derived from the observed and simulated distributions. This approach is usually referred to as

(distributional) bias correction and includes several variants of the quantile mapping (QQM hereinafter) as the most popular techniques (see *Teutschbein and Seibert* [2012], *Gutjahr and Heinemann* [2013], and *Sunyer Pinya et al.* [2015] for a review). However, a number of limitations have been recently reported for these methods. One important drawback of QQM is that it can modify the raw climate change signal [*Hagemann et al.*, 2011; *Pierce et al.*, 2013; *Maraun*, 2013; *Maurer and Pierce*, 2014; *Cannon et al.*, 2015; *Dosio*, 2016]. Also, QQM is not able to correct for biases related to model error in large-scale circulation [*Eden et al.*, 2012; *Addor et al.*, 2016] or heterogeneous biases in space [*Maraun and Widmann*, 2015], and, importantly, QQM is not effective in cases where the observations and RCM outputs have different spatial resolutions, i.e., when downscaling is also required [*White and Toumi*, 2013; *Maraun*, 2013; *Teutschbein and Seibert*, 2013].

As an alternative to these popular techniques, a number of event-wise MOS methods which use the temporal correspondence between simulations and observations have been recently developed, e.g., conditioning the distribution-wise methods to different weather types [*Wetterhall et al.*, 2012] or considering RCM simulations nudged to (or driven by) reanalysis data to train the statistical methods using the temporal correspondence (between simulations and observations) existing in this case [*Turco et al.*, 2011; *Eden et al.*, 2014]. Although the temporal correspondence is weaker for reanalysis-driven RCM climate simulations (driven only at the boundaries of the simulation domain) than for the (grid or spectral) nudged ones, the former simulations are those currently available in most of the international downscaling initiatives—such as Ensemble-based Predictions of Climate Changes and their Impacts (ENSEMBLES) [*van der Linden and Mitchell*, 2009], North American Regional Climate Change Assessment Program (NARCAP) [*Mearns et al.*, 2012], and CORDEX [*Giorgi et al.*, 2009; *Jacob et al.*, 2014]—and, therefore, they can be more widely applied in practice.

Turco et al. [2011] introduced a MOS downscaling method based on the application of the analog technique to the reanalysis (ERA40)-driven RCM outputs from the ENSEMBLES project. They showed that the application of this methodology (hereafter referred to as MOS-Analog) improves the representation of the mean regimes, the seasonal cycle, the frequency and the extremes of precipitation for all the RCMs. It is worth noting that the main advantages of the analog methodology are that (i) it is conceptually simple and easy to implement with low computational cost, (ii) is able to reproduce nonlinear relationship between predictors and predictands, and (iii) can reproduce realistic and spatially coherent precipitation patterns. The main drawback is that it cannot simulate unobserved weather patterns, and this limitation should be cautiously taken into account for climate change studies [see, e.g., *Gutiérrez et al.*, 2013].

In this paper we analyze the application of the MOS-Analog method to downscale future RCM projections. To this aim, we consider the different GCM-RCM combinations available from the ENSEMBLES projects for both the historical (20C3M) and future (A1B) emission scenarios, together with the corresponding reanalysis-driven RCM simulations. First, we evaluate the performance of the method in a control historical period, showing that it can satisfactorily reproduce the observed spatial and temporal climate patterns of mean and extreme precipitation. Second, we analyze the downscaled climate change signal as compared with that corresponding to the direct RCM output for different future periods (2011–2040, 2041–2070, and 2071–2100). Overall, similar regional climate change signals are observed, particularly in cases with a strong signal agreement among members.

The domain of study is the Spanish Iberian Peninsula, which is geographically complex and heterogeneous, and it is characterized by large climate variability due to the influences of different climatological regimes. This is a challenging area for the statistical and dynamical downscaling, since they must be able to simulate very different climates in a relatively small area with notable orographic complexity. *Herrera et al.* [2010] analyzed the performance of the ERA40-driven RCM simulations in this region, showing that they can capture the annual cycle of precipitation in the different river basins. However, they also indicated that some of these models have strong biases and exhibit a poor performance as they overestimate the frequency of rainfall. Moreover, they deficiently represent extreme events. Generally, the MOS-Analog method is able to reduce the biases of these models [*Turco et al.*, 2011]. On the other hand, *Turco et al.* [2013] analyzed the GCM-driven control runs (20C3M scenario) and found large biases for some RCM-GCM combinations attributable to RCM in-house coupling problems with some particular GCMs. Importantly, these biases are shown to distort the corresponding climate change signal. The lessons learned in these previous studies set the basis for the present work.

The study is organized as follows. After this introduction, section 2 describes the RCMs and observational data sets used; section 3 presents the downscaling method, and section 4 analyzes the validation results in a

Table 1. RCM Simulations Produced in the ENSEMBLES Project Used in This Study With the Corresponding Driving GCM^a

Number - Acronym	RCM	Driving GCM	Reference
1 - CNRM ^b	ALADIN	ARPEGE	<i>Radu et al. [2008]</i>
2 - DMI ^b	HIRHAM	ARPEGE	<i>Christensen et al. [2008]</i>
3 - DMI-BCM	HIRHAM	BCM	<i>Christensen et al. [2008]</i>
4 - DMI-ECHAM5	HIRHAM	ECHAM5-r3	<i>Christensen et al. [2008]</i>
5 - ICTP ^b	RegCM3	ECHAM5-r3	<i>Pal et al. [2007]</i>
6 - KNMI ^b	RACMO	ECHAM5-r3	<i>Van Meijgaard et al. [2008]</i>
7 - HC ^b	HadRM3Q0	HadCM3Q0	<i>Haugen and Haakensatd [2006]</i>
8 - MPI ^b	M-REMO	ECHAM5-r3	<i>Jacob [2001]</i>
9 - SMHI ^b	RCA	ECHAM5-r3	<i>Samuelsson et al. [2011]</i>
10 - SMHI-BCM	RCA	BCM	<i>Samuelsson et al. [2011]</i>

^aThe numbers are used to facilitate the reading of the Taylor diagrams presented later (see section 4).

^bThe best performing models in this region according to previous studies [*Herrera et al., 2010; Turco et al., 2013*].

control period. Finally, section 5 analyzes the projection results and section 6 synthesizes the main results of this study.

2. Observed and Simulated Data

2.1. ENSEMBLES RCM Data Set

The EU-funded project ENSEMBLES [*van der Linden and Mitchell, 2009*] was a collaborative effort of different European institutions focused on the generation of climate change scenarios over Europe. Regional simulations were produced with the latest generation RCMs at that time over a common area covering the entire continental European region with a common resolution of 25 km. The resulting data set is publicly available for research activities (<http://ensemblesrt3.dmi.dk>).

A first experiment was carried out using the ERA40 reanalyses from the European Centre for Medium Range Weather Forecasts (ECMWF) [*Uppala et al., 2005*] as boundary conditions for the RCMs. All RCMs were run over a common period of 40 years, 1961–2000.

A second experiment for climate change studies was done using different GCM simulations over two periods: A control one using the 20C3M scenario (1961–2000), i.e., with observed greenhouse gasses, and a future one based on the A1B scenario (2001–2100), which is consistent with the emission trend over recent decades [*Peters et al., 2012*].

For this study we consider the 10 RCMs available in the ENSEMBLES archive that cover the period until 2100 (Table 1). For practical reasons, the daily outputs of the RCMs were bilinearly interpolated from their original resolution (25 km) to the grid defined by *Spain02* (20 km approximately) described in the next section.

2.2. Observed Data

The observed data are the high-resolution (0.2° × 0.2°, 20 km × 20 km approximately) gridded data set *Spain02* [*Herrera et al., 2012, 2016*] of daily precipitation over Spain. This recently developed data set—which is publicly available for research activities at <http://www.meteo.unican.es/datasets/spain02>,— was produced using data from 2756 quality-controlled stations from the Spanish Meteorological Agency (AEMET), covering the Spanish Iberian Peninsula and the Balearic Islands over the period 1950–2008 (see Figure 1).

An analysis of upper percentiles and extreme indicators revealed the capability of *Spain02* to reproduce the intensity and spatial variability of extremes [*Herrera et al., 2012*]. The high quality of this data set has been confirmed also by *Turco and Llasat [2011]*, and it has been used to validate [*Herrera et al., 2010; Gómez-Navarro et al., 2012*], post process [*Turco et al., 2011*], and apply [*Turco et al., 2014*] the ENSEMBLES RCMs described in section 2.1.

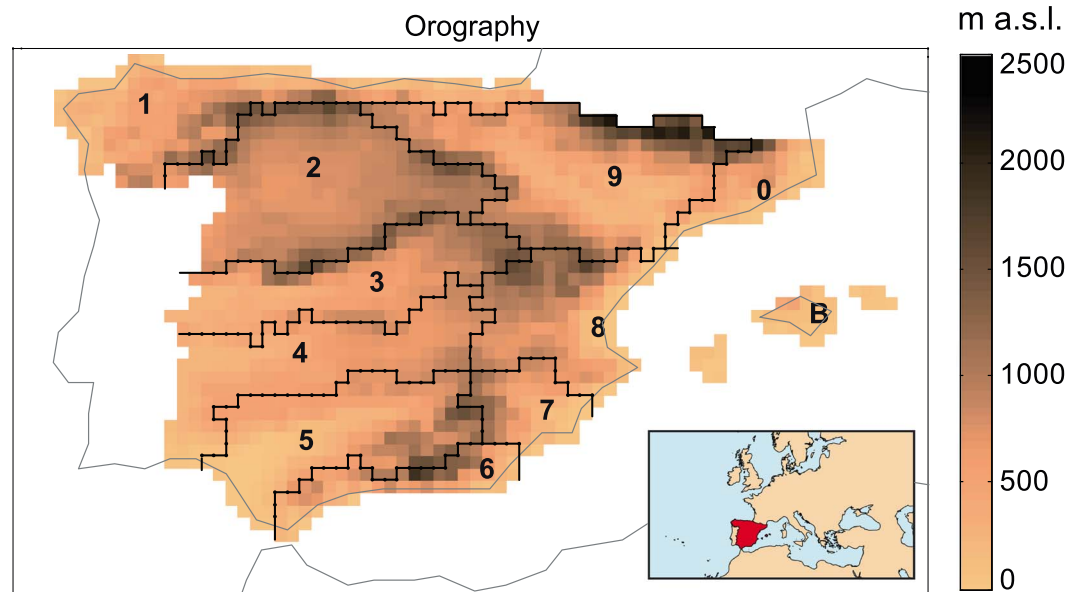


Figure 1. Topography of Spanish Iberian Peninsula and the Balearic Islands as represented by Spain02 at $0.2^\circ \times 0.2^\circ$, showing the main river basins: (0) Catalana, (1) Norte, (2) Duero, (3) Tajo, (4) Guadiana, (5) Guadalquivir, (6) Sur, (7) Segura, (8) Levante, (9) Ebro, and (B) Baleares. The inset shows a geographical map at larger scale.

3. Methodology

3.1. MOS Based on Analogs: MOS-Analog

The analog method [Lorenz, 1963, 1969] is based on the hypothesis that “analog” atmospheric patterns (predictors) should cause “analog” local effects (predictands). This is one of the most popular downscaling techniques and has been used in many applications [see, e.g., Zorita *et al.*, 1995; Matulla *et al.*, 2008; Gutiérrez *et al.*, 2012; Radanovics *et al.*, 2013].

The predictand used in this paper is the interpolated 0.2° observed precipitation over the Iberian Peninsula given by Spain02, whereas the RCM-simulated precipitation field is used as predictor. Note that this variable is one of the most informative variables for precipitation downscaling purposes [Eden *et al.*, 2012], but generally it is avoided in perfect prognosis downscaling studies (e.g., precipitation is not used per se as predictor) since it is very model dependent [see, e.g., Jerez *et al.*, 2013], and thus, there may be significant differences between the reanalysis and the GCMs. This problem does not exist in the MOS setting. Indeed, the RCM precipitation is used both for training (considering the ERA40-driven simulations) and for test or future periods (considering the GCM-driven simulations), allowing us to define a simple and parsimonious method. Therefore, the predictor pattern considered in this paper is defined by the RCM precipitation in a 0.2° grid covering the Iberian Peninsula (see Turco *et al.* [2011], or more details on the sensitivity of the method to different configurations).

The MOS-Analog downscaling consists of two main steps, which are repeated for each day to be downscaled (see Figure 2):

1. For each daily precipitation pattern $A(t)$ from the GCM-driven RCM simulation (from a control or future scenario run), the closest precipitation pattern of the ERA40-driven simulation $B(t')$ in the historical period is obtained based on the Euclidean distance between both fields.
2. Then, the precipitation $b(t')$ observed during this analog historical date t' is assigned as the downscaled value $a(t)$ for the GCM-driven RCM.

Note that, as a result of this process, the method can only generate values which have been observed in the historical period and, therefore, this limitation can affect its extrapolation capability in future climate change simulations, particularly for extreme values [Gutiérrez *et al.*, 2013].

3.2. Quantile Mapping Method: QQM

We use the popular parametric quantile mapping method introduced by Piani *et al.* [2010], including the frequency adaptation proposed by Themeßl *et al.* [2012] (hereafter QQM). This method assumes that both

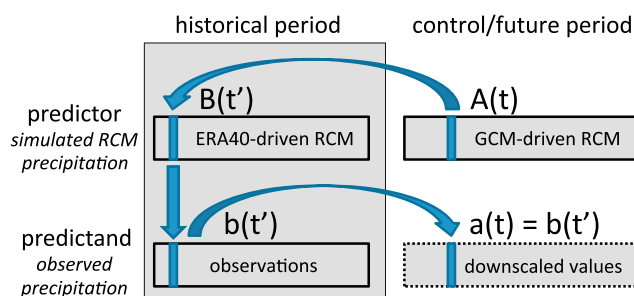


Figure 2. Schematic illustration of the MOS-Analog method (adapted from *Fernandez and Saenz* [2003]). See the text for details.

observed and simulated precipitation intensity distributions are well approximated by the gamma distribution. For the sake of the comparability with the MOS-Analog method, the transfer function has been adjusted considering the ERA40-driven simulation and applied to calibrate the GCM-driven simulation for both the historical 20C3M (1961–2000) and future A1B (2001–2100) scenarios as follows:

$$X_{GCM}^* = F_{Obs}^{-1}(F_{ERA40}(X_{GCM})), \tag{1}$$

where X_{GCM} and X_{GCM}^* are the original and corrected values of the GCM-driven simulation, and F_{Obs} and F_{ERA40} the adjusted Gamma distribution of the observations and the ERA40-driven simulation. Note that, in the standard application of these techniques, the adjustment is done considering the historical GCM driven simulations.

3.3. Comparison Measures

Three main approaches have been applied to evaluate the applicability of the MOS-Analog approach. First, we compare the simulated (both RCM outputs and MOS downscaled ones) and observed climatologies (spatial patterns) for the precipitation indices shown in Table 2 computed from daily data and characterizing total precipitation, dry and wet spells, and extreme precipitation, as defined by the joint CCI/CLIVAR/JCOMM Expert Team on Climate Change Detection and Indices (ETCCDI indices) [*World Meteorological Organization, 2009; Zhang et al., 2011*]. The comparisons between the simulated and observed climatologies are summarized using Taylor diagrams [*Taylor, 2001*]. This diagram synthesizes three spatial measures—standard deviation (S), centered root-mean-square difference (R), and correlation (C)—in a single bidimensional plot. Two variations from the standard Taylor diagram have been applied in this study:

1. The measures S and R are normalized, dividing them by the standard deviation of the observations. In this way it is possible to compare the different indices.
2. Information about spatial average of the bias (M) has been introduced (using colors) for each point in the Taylor diagram. In particular, we use the difference between the simulated and observed mean, normalized by the observed mean.

Second, in order to assess the correspondence of the simulated and observed annual cycles, we analyze the performance of the method in the different river basins (according to Figure 1) at a monthly scale. To this aim, we calculated several monthly indices spatially averaged for each river basin. These standard measures

Table 2. Climatic Mean and Extreme ETCCDI Indices for Precipitation Used in This Work (See Also <http://etccdi.pacificclimate.org>)

Label	Description	Units
<i>PRCPTOT</i>	Total precipitation	mm
<i>R1</i>	Number of day with precipitation over 1 mm/d	days
<i>SDII</i>	Mean precipitation amount on a wet day (>1 mm)	mm
<i>R20</i>	Number of days with precipitation over 20 mm/d	days
<i>RX1DAY</i>	Maximum precipitation in 1 day	mm
<i>CDD</i>	Consecutive dry days (<1 mm)	days
<i>CWD</i>	Consecutive wet days (>1 mm)	days

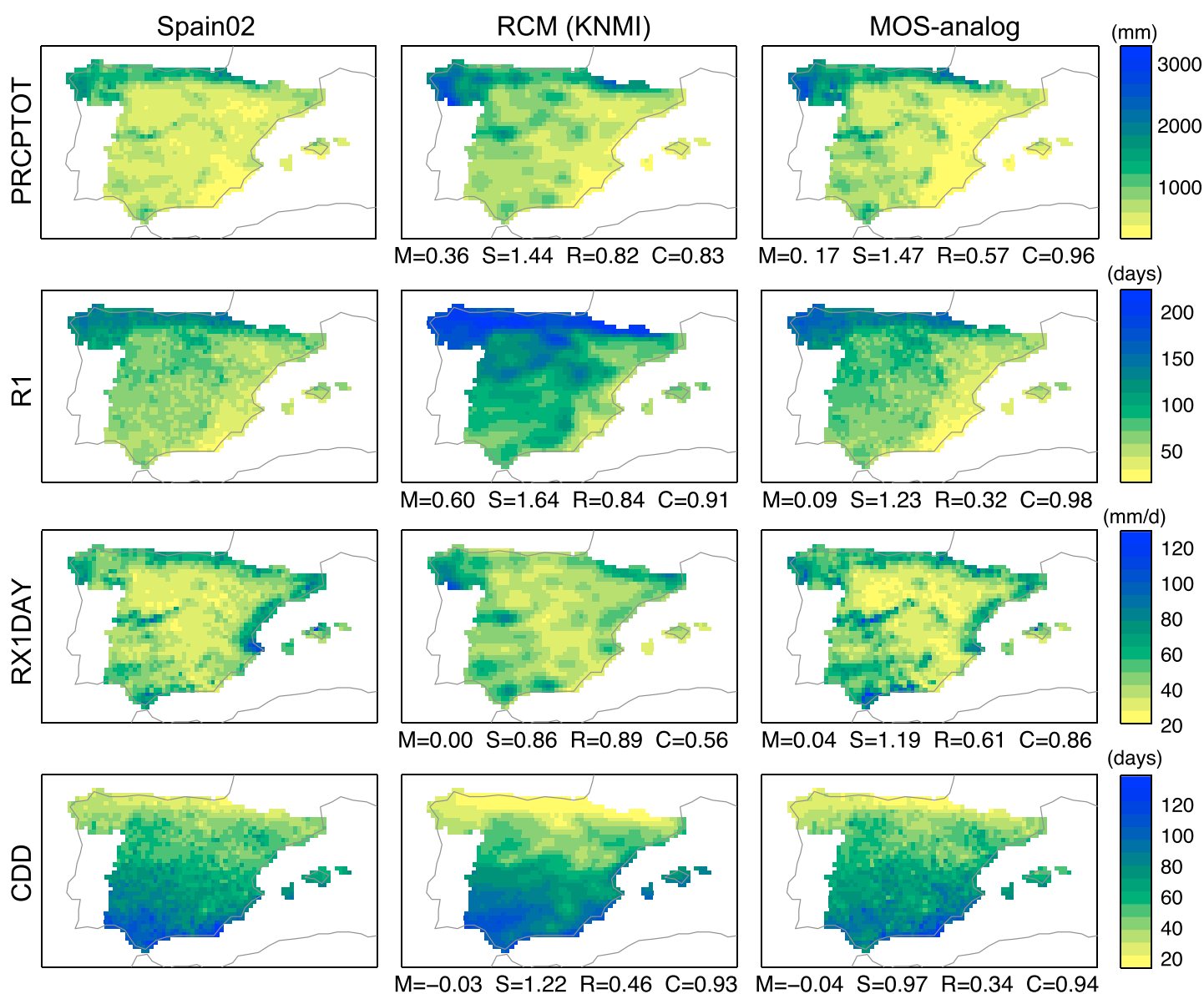


Figure 3. Spatial distribution of the observed (left column) Spain02, (middle column) RCM, and (right column) MOS-Analog mean values (averaged over the baseline period 1971–2000) for some of the precipitation indices shown in Table 2. The spatial validation scores for the RCM and MOS-Analog simulated values are given below the corresponding panels: mean error M (in % with respect to the observed mean); the relative standard deviation S ; the centered root-mean-square R ; and the correlation C .

(both regarding the spatial patterns of the precipitation climatologies and considering the annual cycle) have been calculated over the period 1971–2000, which is later used to estimate the climate change signal (i.e., the difference between the downscaled values for the future A1B period and the control 20C3M ones).

Finally, we analyze how well the MOS-Analog downscaled results preserve the climate change signal of the RCMs (see section 5 for more details). In order to assess this consistency, and for the sake of comparison with standard bias correction techniques, we compare the results of the MOS-Analog method with those resulting from the popular bias correction quantile mapping technique described in section 3.2.

In order to graphically show both the climate change signal and the ensemble agreement, we have adopted the technique used in Hemming *et al.* [2010], in which the map combines the ensemble mean scenario, with different colors, and the percentage agreement in the direction of change among the ensemble members, with different intensity of colors [Kaye *et al.*, 2012].

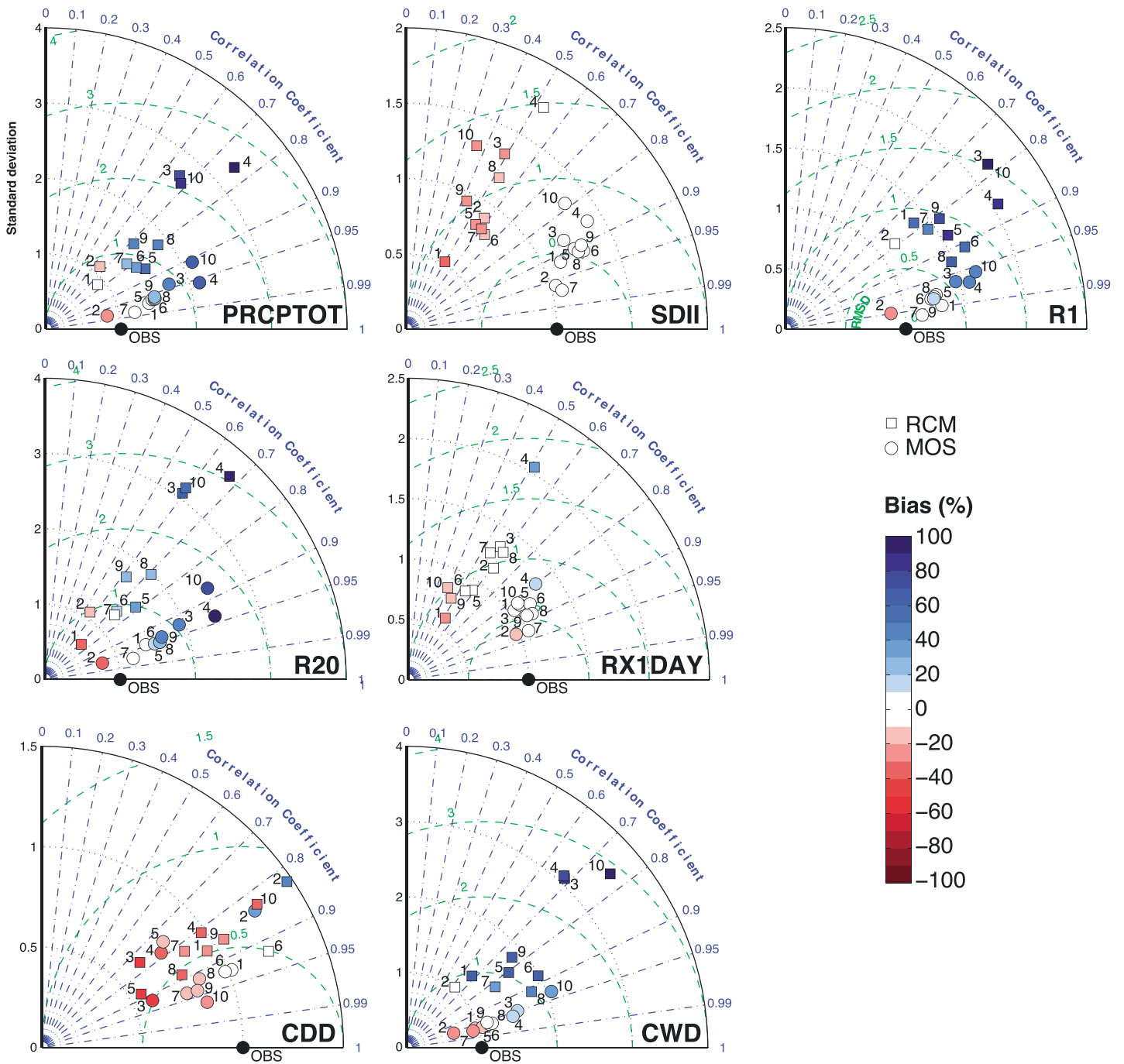


Figure 4. Taylor diagrams for the GCM-driven RCMs for different ETCCDI indices (Table 2). The squares and the dots with the numbers indicate, respectively, the model output (as referred on Table 1) and the MOS-Analog applied to this model.

4. Validation Results in the Control Period

In this section we analyze the results obtained when downscaling the historical (20C3M) GCM-driven RCMs in the control period 1971–2000.

4.1. Maps of Mean and Extreme Climates

As an illustrative example, and for the sake of brevity, in Figure 3 we show the comparison maps for the KNMI model and the corresponding MOS-Analog values; note that this RCM has been chosen since it is one of the most skilful for precipitation in this region [Herrera et al., 2010], thus could be more challenging for the MOS

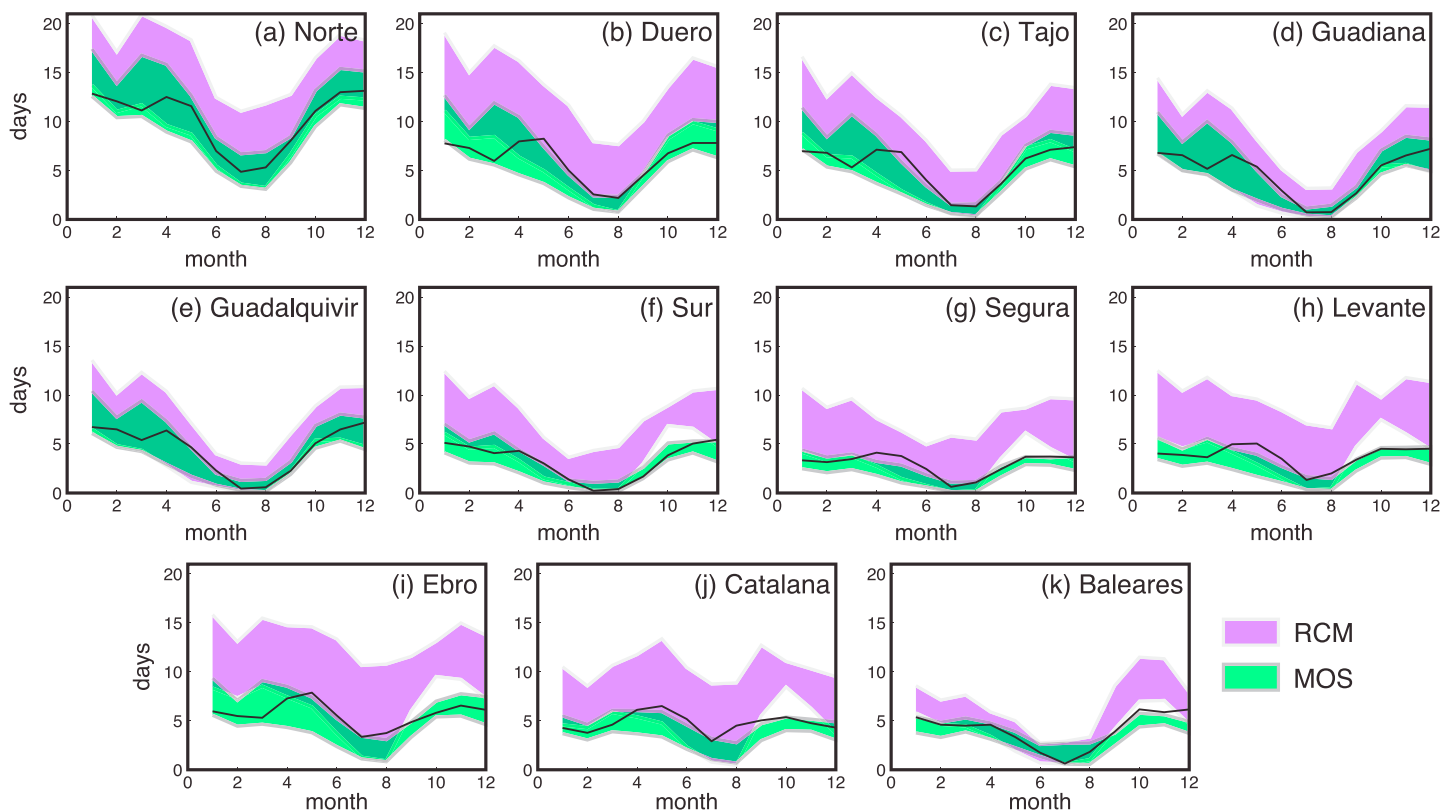


Figure 5. Seasonal cycle of the spatially averaged $R1$ index (in days) for each river basin (according to Figure 1). The black line represents the observed (Spain02) climatology. The violet-shaded band spans the values for the RCMs, while the green one spans the respective MOS downscaled values.

method to improve it. The panels in this figure show the annual values of the indices (averaged over the common period 1971–2000) for the observations (Spain02, Figure 3, left column), the regional KNMI simulations (Figure 3, middle column), and the corresponding MOS-Analog downscaled values (Figure 3, right column); the numbers below the panels in this figure indicate the bias (or mean error, M), the relative standard deviation (S), the centered root-mean-square (R), and the correlation (C). These metrics are then used to produce a Taylor diagram summarizing this information. This figure shows that the MOS-Analog downscaled values clearly outperform the raw RCM outputs. The Taylor diagrams shown in Figure 4 summarize the verification results for all the models and indices in the control period (1971–2000).

These figures show that, overall, the MOS-Analog method improves considerably the RCM results for all the indices (less evident for the CDD index, as already noticed by Turco *et al.* [2011]), with larger spatial correlation values and standard deviation closer to the observed ones. In terms of errors, the MOS-Analog downscaling method also improves the RCMs results for the bias (M) and the centered root-mean-square error (R). In particular, the MOS-Analog clearly reduces their overestimation of rainfall frequency, common on the RCMs as they tend to drizzle [Gutowski *et al.*, 2003], correcting partially their underestimation of CDD while the bias for CWD shifts from RCM positive values to MOS-Analog positive or negative values depending on the RCM. Finally, although the MOS-Analog is able to reduce the overestimation of $R20$, $R1$, and $PRCPTOT$ given by the RCMs, there is yet a positive bias for these indicators which could affect the future climate change signal. These results are generally confirmed also repeating this analysis for each subregions of Figure 1 (Figures S1–S7 in the supporting information).

Overall, the MOS-Analog method is able to improve the above considered scores for different indices for all RCMs, although for the worst-performing models the downscaling is less effective. Note that three GCM-driven RCMs (3. DMI-BCM; 4. DMI-ECHAM5; 10. SMHI-BCM) show significantly worse performance than the other simulations. This result confirms the study of Turco *et al.* [2013], which analyzed a greater ensemble of RCMs from ENSEMBLES containing the 15 models with data up to 2050. They found large biases for some RCM-GCM combinations, and these biases are shown to distort the corresponding climate change signal.

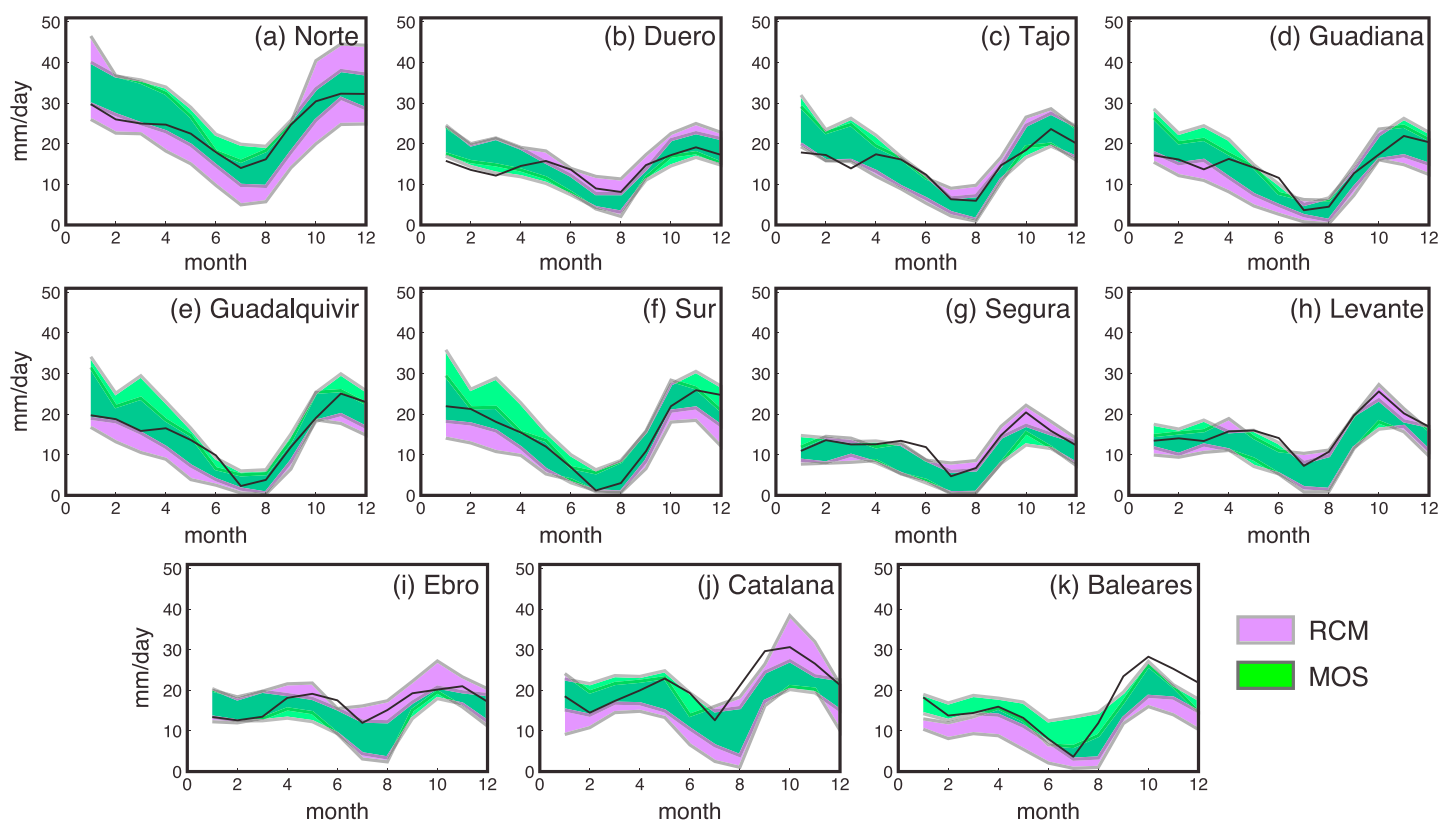


Figure 6. As in Figure 5 but for $RX1DAY$ index (in mm/d).

Therefore, it is not advisable ignoring the performance of the RCM-GCM runs in the control period and the side effects of large biases. Thus, hereafter, we consider the ensemble of the best seven models (Table 1).

4.2. Seasonal Cycle

In this section, we analyze the ability of the RCMs and the MOS-Analog downscaled results to reproduce the strong seasonal cycle of rainfall, which differs considerably among the different river basins (according to Figure 1). Here we focus on a seven-member ensemble formed by the best performing RCMs identified in the previous section. We consider the seasonal cycle of the number of precipitation days ($R1$; Figure 5) and the monthly maximum ($RX1DAY$; Figure 6). Similar results have been found for the total precipitation (Figure S8).

Despite the differences in values, the three indices have a similar cycle among the basins, with two maximum periods in the Mediterranean basin, the major one in autumn and the secondary in spring and, for the remaining basins, a maximum in winter and a minimum in summer. The performance of the RCMs and the MOS-Analog method to reproduce the observed seasonal cycles of the indices, in the different basins, is quite remarkable, with generally a reduced spread (smaller uncertainty) in the latter case (see also Tables S1–S3 for a quantification of the error for each index and each river basin). In particular, as pointed out in the previous section, the RCMs clearly overestimate the $R1$ index and the MOS-Analog is able to correct this problem (Figure 5). Also, it is worth noting the good performance of both the RCMs and the MOS-Analog method to reproduce the observed seasonal cycle of the $RX1DAY$ index (Figure 6). Finally, note that the greater errors are generally found for the Mediterranean basins (Figures 5g–5k and 6g–6k and basins “Segura,” “Levante,” “Ebro,” “Catalana,” and “Baleares” in Tables S1–S3), as also found by *Herrera et al.* [2010] and *Turco et al.* [2011] considering the ERA40-driven RCMs.

5. Future Scenarios

In this section we analyze the regional climate change signals for different future periods (2011–2040, 2041–2070, 2071–2100), obtained as the ratio (expressed as percentage of change) of the mean values for the corresponding A1B GCM-driven RCM simulations and the 20C3M control ones in the baseline

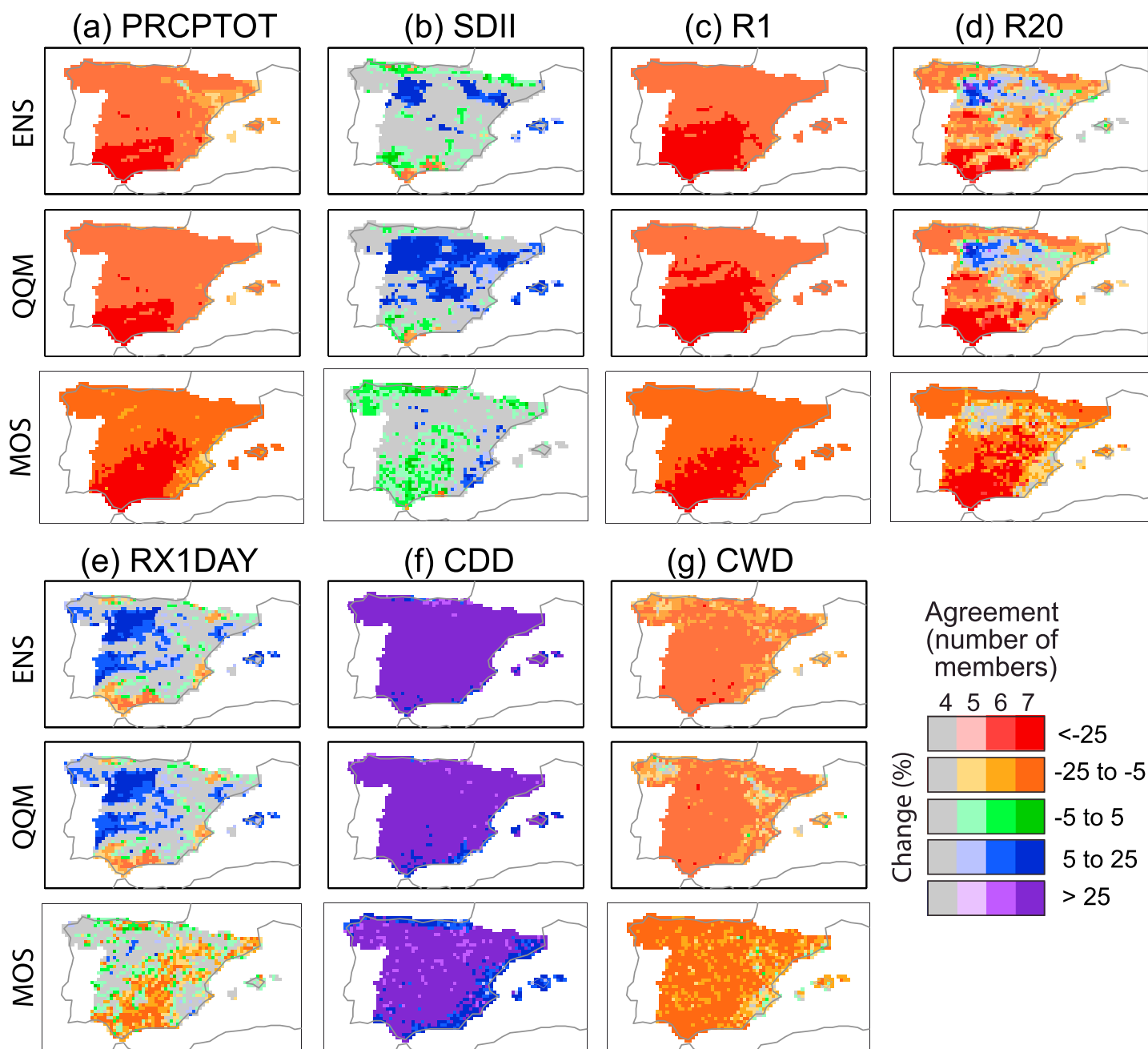


Figure 7. Future climate change signals (expressed as percentage of change with regard the baseline control period 1971–2000) for the period 2071–2100 for the precipitation indices shown in Table 2. The different rows correspond to the results for to the seven-member ensemble (ENS), the quantile mapping bias correction method (QQM), and the MOS-Analog downscaling method. The color saturation level shows the percentage agreement in the direction of change among the ensemble members.

(1971–2000) period. For the sake of comparison with standard bias correction techniques, in addition to the MOS-Analog method, this analysis also includes the results corresponding to the Piani quantile mapping method (QQM).

Figure 7 shows the regional climate change signal for all indices shown in Table 2 for the future period 2071–2100 for the seven-member (see Table 1) RCM ensemble (ENS), together with results for the MOS-Analog downscaling method (MOS) and the quantile mapping method (QQM). High agreement for the RCM climate change signals appears in most of the Iberian Peninsula for the indices *PRCPTOT*, *R1*, and *CWD* (with negative changes), and for the index *CDD* (with positive changes, larger than +25%). Instead, the other

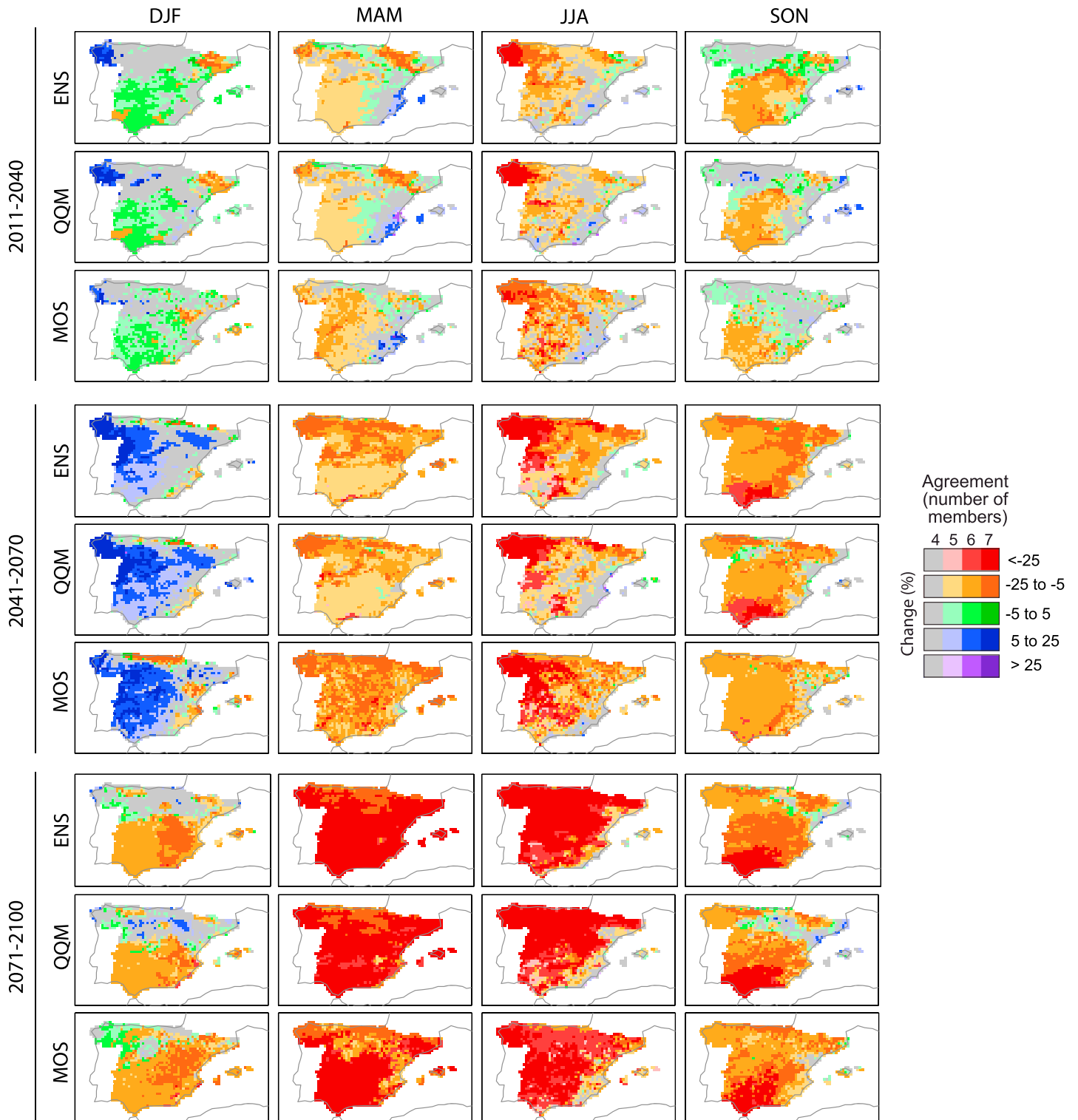


Figure 8. Seasonal changes of the precipitation index $PRCP_{TOT}$ for different future periods (2011–2040, 2041–2070, 2071–2100). Values for MOS-Analog (MOS), the quantile mapping bias correction method (QQM), and RCMs (ENS) are expressed in percentage of change between the baseline (1971–2000) and future periods. The color saturation level shows the percentage agreement in the direction of change among the ensembles.

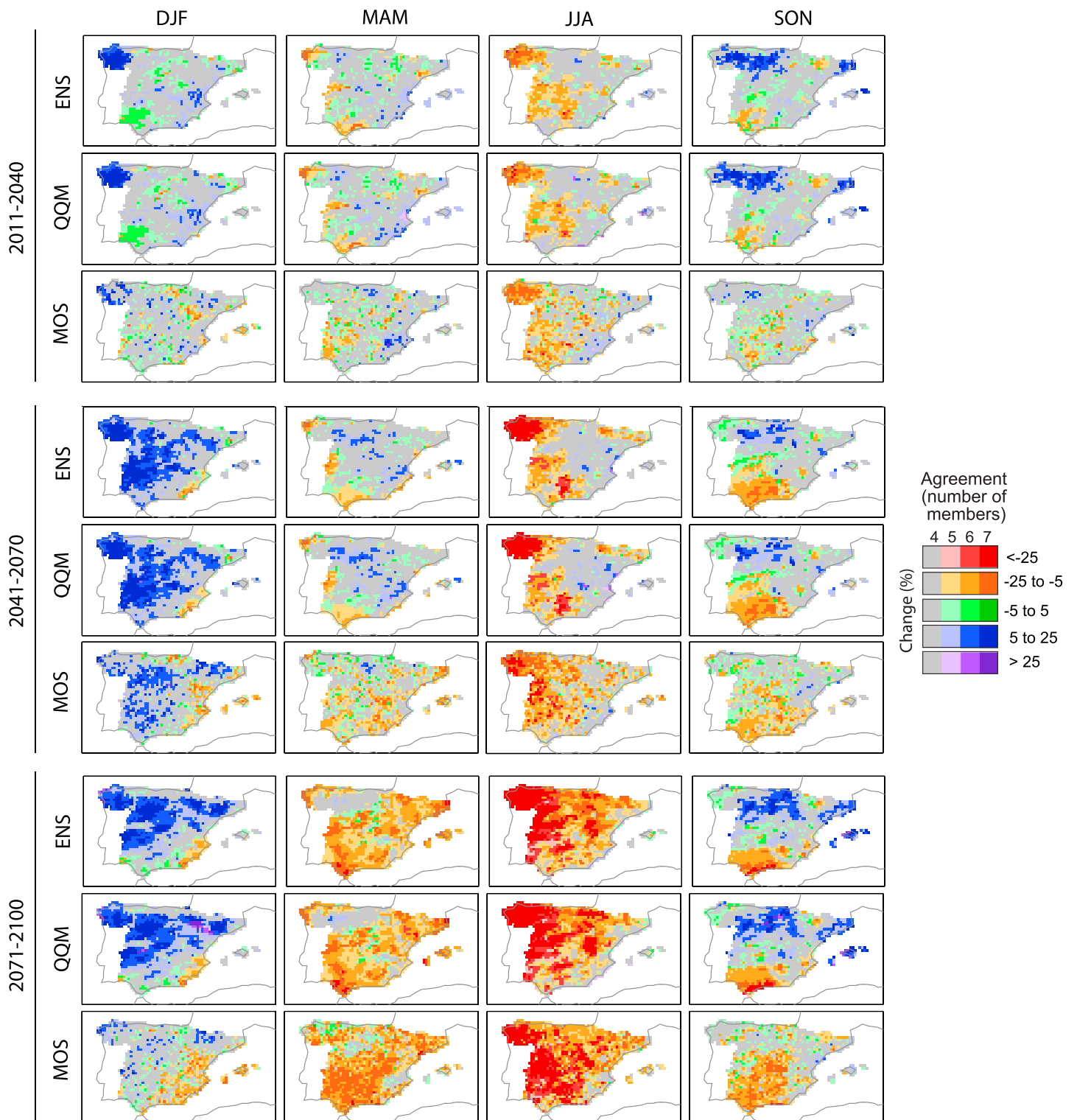


Figure 9. The same as Figure 8 but for RX1DAY index.

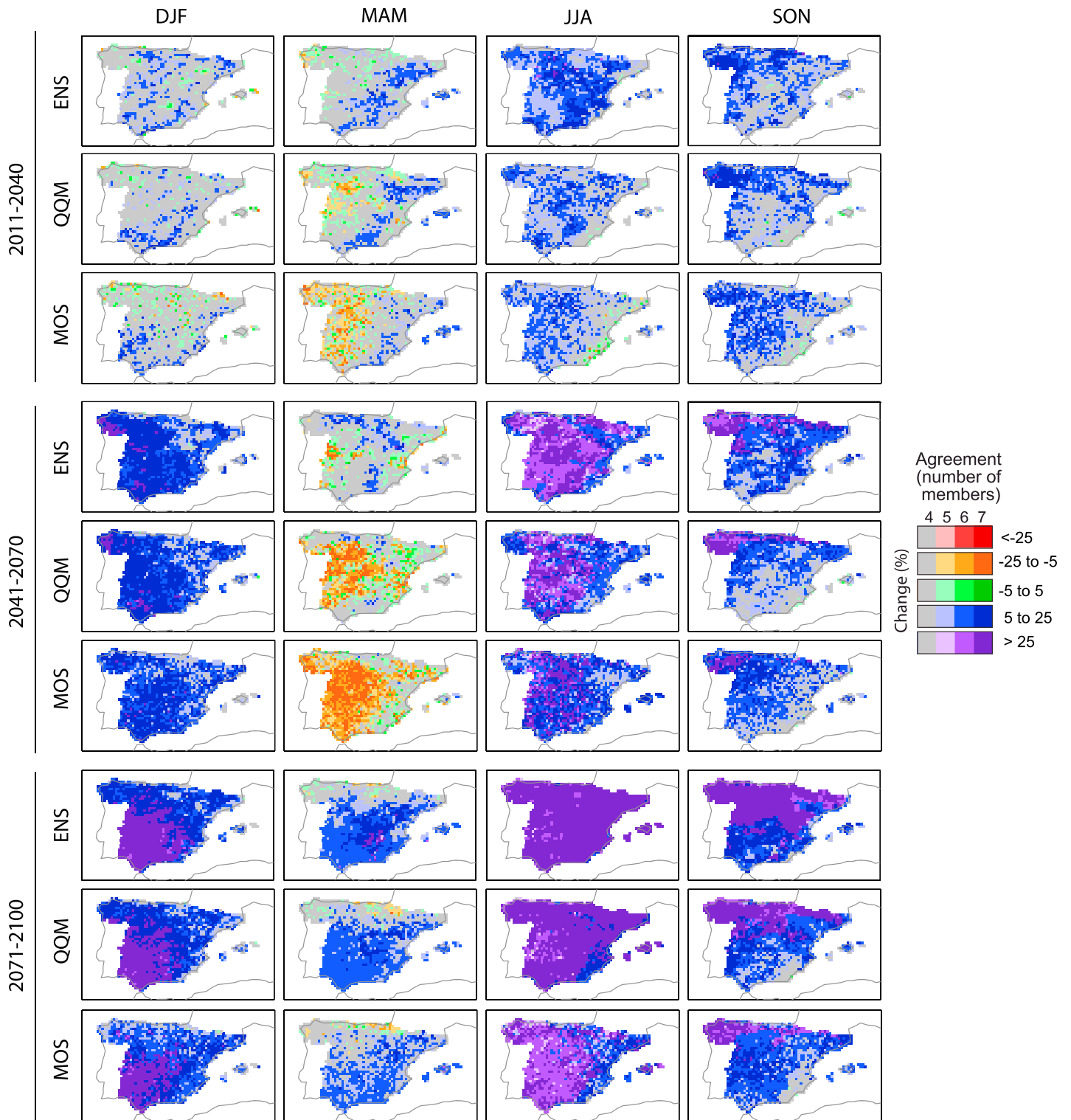


Figure 10. The same as Figure 8 but for CDD index.

indices display more heterogeneous signals (with large areas either positive or negative) and more disagreement between the models. For instance, for the *SDII* and *RX1DAY* indices, large part of the maps show no agreement among the RCMs.

Overall, the RCM regional climate change signal for the different indices is preserved by the QQM, with the exception of *SDII*, where the QQM exhibits a larger region with positive signal. These differences are probably due to the use of the reanalysis-driven RCM outputs to calibrate the bias correction method—for the sake of comparability with the MOS-Analog method—and are induced by the difference of rain frequencies in the reanalysis- and control-driven simulations. Note that the standard application of the QQM method (using the control simulations for calibration) could reduce this disagreement. On the other hand, the MOS-Analog method broadly preserves the climate change signal for nonextreme indices but exhibits large differences for *R20* and *RX1DAY*, particularly for those regions with positive signals. This could be a result of the limitation of the analog method to extrapolate unobserved values, particularly for the *RX1DAY* results. Overall, similar conclusions are obtained for the climate change signals relative to the different periods 2011–2040 and 2041–2070 (see Figures S9 and S10, respectively), although with lower values of changes (in absolute value) and lower level of agreement between the models compared to the pattern shown for the end of the century (Figure 7).

We also explored the seasonal projections for some representative indices for three future A1B periods. Figure 8 shows the seasonal climate change signal for the total precipitation (*PRCPTOT* index). These projections indicate regional changes in the range from –25% to –5% with greater agreement in spring, summer, and autumn (March–April–May (MAM), June–July–August (JJA), and September–October–November (SON), respectively), mostly in the West of the region, for the end of the century. Interestingly, in the Mediterranean coast the agreement in JJA is small even for the last period. The winter (December–January–February, DJF) projections show large fluctuations in the direction of change, from mainly negative in the first period, 2011–2040, to mainly positive in 2041–2070, and again negative in 2071–2100. This is also the season with large areas of the maps with no agreement on the sign of the changes.

Figure 9 considers the *RX1DAY* index and shows a quite heterogeneous pattern, with low level of agreement, although there are some areas with consistent pattern of positive changes (between 5% and 25%) in DJF, and negative (between –25% and –5%) in the other seasons, mainly in summer (with changes even lower than –25%). Generally, higher agreement is found for the end of the century.

Finally, Figure 10 suggests a high agreement in the increase in the *CDD* index (i.e., longer periods without rain), especially for the period 2071–2100, with most of the area agreeing on more than 25% of change, regardless of the considered season. It is worth noting that for the period 2041–2070, both the QQM and the MOS-Analog methods show a negative change over most of the domain, while ENS displays low level of agreement among the RCMs.

6. Summary and Conclusions

The present study has investigated (i) the potential of the recently introduced MOS-Analog downscaling method for climate change projections when applied to RCM precipitation outputs and (ii) how well the method preserves the RCM climate change signal for a set of precipitation indices. The analysis focuses on precipitation over Spain and, besides the MOS-Analog method, a standard distributional-based quantile mapping approach is also considered for comparison purposes.

The validation against the observed gridded data Spain02 shows that the MOS-Analog method clearly outperforms the raw RCM outputs in the control period (20C3M scenario). Specifically, the MOS-Analog downscaling method improves considerably the RCM results for all the indices considered, although for the worst-performing models (DMI-BCM, DMI-ECHAM5, and SMHI-BCM) the downscaling method is less effective. These RCMs have very large biases and can be considered outliers/errors of the ensemble [Turco *et al.*, 2013].

The projected changes are quite consistent among the RCMs for total precipitation, wet-day frequency and spell indices. High level of consistency in the geographical patterns are found for all the seasons, except for winter toward the end of the century. In particular, the higher agreement between models in the later period could be due to a relative smaller influence of natural variability toward the end of the century. The main drivers of these projections are probably the synoptic structures that drive the decreasing precipitation (e.g., persistence of anticyclones) [Sumner *et al.*, 2003; García-Valero *et al.*, 2012; Cortesi *et al.*, 2014] and the

land-surface atmosphere interactions (e.g., soil moisture feedbacks) [Seneviratne et al., 2010; Jerez et al., 2012]. Our confidence in the physical mechanism and the model results gives some credibility to the increasing drought risk in the Mediterranean region [Orlowsky and Seneviratne, 2011; Dai, 2011]. In spite of the agreement of the projected changes for total precipitation, wet-day frequency, and spell indices, the overall uncertainties in heavy rainfall climate projections remain quite large, even for the end of the century. Indeed, due to the importance of the convective process for intense rainfall in this region [Llasat, 2001; Llasat et al., 2014] and the common weakness of the models to simulate these processes [Hohenegger et al., 2008; Rowell, 2011], the heavy rainfall projections should be taken with caution [Kendon et al., 2014]. There is also a large uncertainty for extreme indices ($R20$ and $RX1DAY$) with large regions with negative and positive signals.

The RCM climate change signal is broadly preserved by the distributional-based quantile mapping method, with some differences mainly for $SDII$ due to the procedure used to calibrate the model (using reanalysis-driven RCM data, for the sake of comparability with MOS-Analog results) and to the different wet-day frequencies of the reanalysis- and control-driven RCM simulations. The MOS-Analog method also broadly preserves the climate change signal with the exception of extreme indices ($R20$ and $RX1DAY$ in this work). This is probably due to the limitation of the MOS-Analog method to simulate unobserved records. This could make this method unsuitable to downscale climate change projections for those applications where extreme values are important. However, it is worth noting that this method can produce accumulated values or frequencies over several days larger (or smaller) than the historical values and, therefore, can extrapolate nonobserved values for these types of indices. Finally, it must be noted that standard bias correction methods are not intended to correct climate trends [Maraun, 2016], and methods that deliberately constrain the climate change signals based on process understanding are rare [Collins et al., 2012; Walton et al., 2015]. In this study, the cases where the MOS-Analog method modifies the RCM climate signals (for extreme indices) could be simply explained by the limitation of the method to extrapolate unobserved values (e.g., higher extremes simulated by the RCM for a future period) and not by a merit of the method to introduce plausible changes in the regional climate change signal—which could be the case in other situations, since the MOS-Analog can potentially introduce extra regional information in the downscaling process.

In the case of the MOS-Analog method, since the analog search is performed at a national level, the down-scaled values preserve the spatial coherence of the observed fields. Therefore, this method can be considered a spatially consistent alternative for distributional bias correction methods. Moreover, it could be easily extended to a multivariable consistent framework by defining joint patterns (e.g., precipitation-temperature) for the analog search.

Finally, we underline that bias correction remains a provisional solution until better models will be available (see Ehret et al. [2012], Pielke and Wilby [2012], and Maraun [2016], and references therein for a critical review on the bias correction techniques). It is worth noting that a newer generation of climate models are now available (developed in the framework of the CORDEX program), with up-to-date RCMs, but still affected by biases [Kotlarski et al., 2014; Jerez et al., 2015]. The application of the MOS-Analog method to these RCMs remains to be done.

To sum up, the results shown in this paper suggest that the increasing dryness could be considered a robust result and indicate the urgency to apply adaptation and mitigation strategies, according to the Spanish National Climate Change Adaptation Plan (www.magrama.gob.es/es/cambio-climatico/temas/impactos-vulnerabilidad-y-adaptacion/), also considering that, already at present, many areas in Spain suffer from problems related to water resources [Quiroga et al., 2011]. The MOS downscaled data are freely available for research purposes by applying to the corresponding author.

References

- Addor, N., M. Rohrer, R. Furrer, and J. Seibert (2016), Propagation of biases in climate models from the synoptic to the regional scale: Implications for bias adjustment, *J. Geophys. Res. Atmos.*, 121, 2075–2089, doi:10.1002/2015JD024040.
- Cannon, A. J., S. R. Sobie, and T. Q. Murdock (2015), Bias correction of GCM precipitation by quantile mapping: How well do methods preserve changes in quantiles and extremes?, *J. Clim.*, 28(17), 6938–6959.
- Ceglar, A., A. Toreti, R. Lecerf, M. Van der Velde, and F. Dentener (2016), Impact of meteorological drivers on regional inter-annual crop yield variability in France, *Agric. For. Meteorol.*, 216, 58–67.
- Christensen, J. H., F. Boberg, O. B. Christensen, and P. Lucas-Picher (2008), On the need for bias correction of regional climate change projections of temperature and precipitation, *Geophys. Res. Lett.*, 35, L20709, doi:10.1029/2008GL035694.
- Christensen, O., M. Drews, J. Christensen, K. Dethloff, K. Ketelsen, I. Hebestadt, and A. Rinke (2008), The HIRHAM regional Climate Model version 5, *Tech. Rep. 06-17*, DMI, Copenhagen, Denmark. [Available at <http://www.dmi.dk/dmi/en/print/tr06-17.pdf>.]

Acknowledgments

This work was partially supported by the strategic action for energy and climate change by the Spanish R+D 2008–2011 Program ESTCENA (code 200800050084078), the project MULTI-SDM (CGL2015-66583-R, MINECO/FEDER), the Italian project of Interest NextData of the Italian Ministry for Education, University and Research, and by the European Science Foundation within the framework of COST ES1102 (Validating and integrating downscaling methods for climate change research). This paper has also been written under the framework of the International HYMEX project and the Spanish HOPE (CGL2014-52571-R) project. We also acknowledge the ENSEMBLES project (funded by the European Commission's 6th Framework Programme through contract GOCE-CT-2003-505539) for the RCM data used in this work (<http://ensemblesrt3.dmi.dk/>). The authors thank AEMET and UC for the data provided for this work (Spain02 gridded precipitation data set, www.meteo.unican.es/es/datasets/spain02). Special thanks to the authors of the MeteoLab-Toolbox (www.meteo.unican.es/software/meteolab) which helped us to postprocess the data and to validate the method. Finally, we thank the anonymous referees for their useful comments.

- Collins, M., R. E. Chandler, P. M. Cox, J. M. Huthnance, J. Rougier, and D. B. Stephenson (2012), Quantifying future climate change, *Nat. Clim. Change*, 2(6), 403–409.
- Cortesi, N., J. C. Gonzalez-Hidalgo, R. M. Trigo, and A. M. Ramos (2014), Weather types and spatial variability of precipitation in the Iberian peninsula, *Int. J. Climatol.*, 34(8), 2661–2677.
- Dai, A. (2011), Drought under global warming: A review, *Wiley Interdiscip. Rev. Clim. Change*, 2(1), 45–65.
- Dosio, A. (2016), Projections of climate change indices of temperature and precipitation from an ensemble of bias-adjusted high-resolution EURO-CORDEX regional climate models, *J. Geophys. Res. Atmos.*, 121, 5488–5511, doi:10.1002/2015JD024411.
- Eden, J. M., M. Widmann, D. Grawe, and S. Rast (2012), Skill, correction, and downscaling of GCM-simulated precipitation, *J. Clim.*, 25(11), 3970–3984.
- Eden, J. M., M. Widmann, D. Maraun, and M. Vrac (2014), Comparison of GCM- and RCM-simulated precipitation following stochastic postprocessing, *J. Geophys. Res. Atmos.*, 119, 11,040–11,053, doi:10.1002/2014JD021732.
- Ehret, U., E. Zehe, V. Wulfmeyer, K. Warrach-Sagi, and J. Liebert (2012), Hess opinions: “Should we apply bias correction to global and regional climate model data?”, *Hydrol. Earth Syst. Sci.*, 16(9), 3391–3404.
- Fernandez, J., and J. Saenz (2003), Improved field reconstruction with the analog method: Searching the CCA space, *Clim. Res.*, 24(3), 199–213.
- Foley, A. M. (2010), Uncertainty in regional climate modelling: A review, *Prog. Phys. Geog.*, 34(5), 647–670.
- Fowler, H. J., S. Blenkinsop, and C. Tebaldi (2007), Linking climate change modelling to impacts studies: Recent advances in downscaling techniques for hydrological modelling, *Int. J. Climatol.*, 27(12), 1547–1578. General Assembly of the European-Geosciences-Union, Vienna, Austria, Apr. 2006.
- García-Valero, J. A., J. P. Montavez, S. Jerez, J. J. Gómez-Navarro, R. Lorente-Plazas, and P. Jiménez-Guerrero (2012), A seasonal study of the atmospheric dynamics over the Iberian Peninsula based on circulation types, *Theor. Appl. Climatol.*, 110(1–2), 291–310.
- Giorgi, F., and L. Mearns (1991), Approaches to the simulation of regional climate change—A review, *Rev. Geophys.*, 29(2), 191–216.
- Giorgi, F., C. Jones, and G. Asrar (2009), Addressing climate information needs at the regional level: The CORDEX framework, *WMO Bull.*, 58(3), 175–183.
- Gómez-Navarro, J., J. Montávez, S. Jerez, P. Jiménez-Guerrero, and E. Zorita (2012), What is the role of the observational data set in the evaluation and scoring of climate models?, *Geophys. Res. Lett.*, 39, L24701, doi:10.1029/2012GL054206.
- Gutiérrez, J., D. San-Martín, S. Brands, R. Manzananas, and S. Herrera (2012), Reassessing statistical downscaling techniques for their robust application under climate change conditions, *J. Clim.*, 26, 171–188.
- Gutiérrez, J. M., D. San-Martín, S. Brands, R. Manzananas, and S. Herrera (2013), Reassessing statistical downscaling techniques for their robust application under climate change conditions, *J. Clim.*, 26(1), 171–188.
- Gutjahr, O., and G. Heinemann (2013), Comparing precipitation bias correction methods for high-resolution regional climate simulations using COSMO-CLM, *Theor. Appl. Climatol.*, 114(3–4), 511–529.
- Gutowski, W. J., S. G. Decker, R. A. Donavon, Z. Pan, R. W. Arritt, and E. S. Takle (2003), Temporal-spatial scales of observed and simulated precipitation in central U.S. climate, *J. Clim.*, 16(22), 3841–3847.
- Hagemann, S., C. Chen, J. O. Haerter, J. Heinke, D. Gerten, and C. Piani (2011), Impact of a statistical bias correction on the projected hydrological changes obtained from three GCMs and two hydrology models, *J. Hydrometeorol.*, 12(4), 556–578.
- Haugen, J., and H. Haakensatd (2006), Validation of HIRHAM version 2 with 50 km and 25 km resolution, *Tech. Rep. Gen. Tech. Rep. 9*, RegClim, Norwegian Meteorological Institute, Oslo, Norway. [Available at <http://regclim.met.no/results/gtr9.pdf>.]
- Hemming, D., C. Buontempo, E. Burke, M. Collins, and N. Kaye (2010), How uncertain are climate model projections of water availability indicators across the Middle East?, *Philos. Trans. R. Soc. A*, 368(1931), 5117–35.
- Herrera, S., J. Gutiérrez, R. Ancell, M. Pons, M. Frías, and J. Fernández (2012), Development and analysis of a 50-year high-resolution daily gridded precipitation dataset over Spain (spain02), *Int. J. Climatol.*, 32(1), 74–85.
- Herrera, S., J. Fernández, and J. Gutiérrez (2016), Update of the spain02 gridded observational dataset for EURO-CORDEX evaluation: Assessing the effect of the interpolation methodology, *Int. J. Climatol.*, 36(2), 900–908.
- Herrera, S., L. Fita, J. Fernandez, and J. M. Gutierrez (2010), Evaluation of the mean and extreme precipitation regimes from the ENSEMBLES regional climate multimodel simulations over Spain, *J. Geophys. Res.*, 115, D21117, doi:10.1029/2010JD013936.
- Hohengerger, C., P. Brockhaus, and C. Schaer (2008), Towards climate simulations at cloud-resolving scales, *Meteorol. Z.*, 17(4), 383–394.
- Jacob, D. (2001), A note to the simulation of the annual and inter-annual variability of the water budget over the Baltic Sea drainage basin, *Meteorol. Atmos. Phys.*, 77(1–4), 61–73.
- Jacob, D., et al. (2014), EURO-CORDEX: New high-resolution climate change projections for European impact research, *Reg. Environ. Change*, 14(2), 563–578.
- Jerez, S., J. Montavez, J. Gomez-Navarro, P. Jimenez, P. Jimenez-Guerrero, R. Lorente, and J. F. Gonzalez-Rouco (2012), The role of the land-surface model for climate change projections over the Iberian Peninsula, *J. Geophys. Res.*, 117, D01109, doi:10.1029/2011JD016576.
- Jerez, S., J. P. Montavez, P. Jimenez-Guerrero, J. J. Gomez-Navarro, R. Lorente-Plazas, and E. Zorita (2013), A multi-physics ensemble of present-day climate regional simulations over the Iberian Peninsula, *Clim. Dyn.*, 40(11–12), 3023–3046.
- Jerez, S., et al. (2015), The impact of climate change on photovoltaic power generation in Europe, *Nat. Commun.*, 6, 10014.
- Kaye, N. R., A. Hartley, and D. Hemming (2012), Mapping the climate: Guidance on appropriate techniques to map climate variables and their uncertainty, *Geosci. Model Dev.*, 5(1), 245–256.
- Kendon, E. J., N. M. Roberts, H. J. Fowler, M. J. Roberts, S. C. Chan, and C. A. Senior (2014), Heavier summer downpours with climate change revealed by weather forecast resolution model, *Nat. Clim. Change*, 4(7), 570–576.
- Kotlarski, S., et al. (2014), Regional climate modeling on European scales: A joint standard evaluation of the EURO-CORDEX RCM ensemble, *Geosci. Model Dev.*, 7(4), 1297–1333.
- Llasat, M. C. (2001), An objective classification of rainfall events on the basis of their convective features: Application to rainfall intensity in the northeast of Spain, *Int. J. Climatol.*, 21(11), 1385–1400.
- Llasat, M. C., R. Marcos, M. Llasat-Botija, J. Gilabert, M. Turco, and P. Quintana-Seguí (2014), Flash flood evolution in north-western Mediterranean, *Atmos. Res.*, 149, 230–243.
- Llasat, M. C., R. Marcos, M. Turco, J. Gilabert, and M. Llasat-Botija (2016), Trends in flash flood events versus convective precipitation in the Mediterranean region: The case of Catalonia, *J. Hydrol.*, 541, 24–37.
- Lorenz, E. (1963), Deterministic nonperiodic flow, *J. Atmos. Sci.*, 20, 130–141.
- Lorenz, E. (1969), Atmospheric predictability as revealed by naturally occurring analogues, *J. Atmos. Sci.*, 26(4), 636–646.
- Maraun, D. (2013), Bias correction, quantile mapping, and downscaling: Revisiting the inflation issue, *J. Clim.*, 26(6), 2137–2143.
- Maraun, D. (2016), Bias correcting climate change simulations—a critical review, *Curr. Clim. Change Rep.*, 2(4), 211–220.

- Maraun, D., and M. Widmann (2015), The representation of location by a regional climate model in complex terrain, *Hydrol. Earth Syst. Sci.*, *19*(8), 3449–3456, doi:10.5194/hess-19-3449-2015.
- Maraun, D., M. Widmann, J. M. Gutiérrez, S. Kotlarski, R. E. Chandler, E. Hertig, J. Wibig, R. Huth, and R. A. Wilcke (2015), Value: A framework to validate downscaling approaches for climate change studies, *Earth's Future*, *3*, 1–14.
- Maraun, D., et al. (2010), Precipitation downscaling under climate change: Recent developments to bridge the gap between dynamical models and the end user, *Rev. Geophys.*, *48*, RG3003, doi:10.1029/2009RG000314.
- Marzban, C., S. Sandgathe, and E. Kalnay (2006), MOS, perfect prog, and reanalysis, *Mon. Weather Rev.*, *134*(2), 657–663.
- Matulla, C., X. Zhang, X. L. Wang, J. Wang, E. Zorita, S. Wagner, and H. von Storch (2008), Influence of similarity measures on the performance of the analog method for downscaling daily precipitation, *Clim. Dyn.*, *30*(2–3), 133–144.
- Maurer, E. P., and D. W. Pierce (2014), Bias correction can modify climate model simulated precipitation changes without adverse effect on the ensemble mean, *Hydrol. Earth Syst. Sci.*, *18*(3), 915–925, doi:10.5194/hess-18-915-2014.
- Mearns, L. O., et al. (2012), The North American regional climate change assessment program: Overview of phase I results, *Bull. Am. Meteorol. Soc.*, *93*(9), 1337–1362.
- Orlowsky, B., and S. I. Seneviratne (2011), Global changes in extreme events: Regional and seasonal dimension, *Clim. Change*, *110*(3–4), 669–696.
- Pal, J. S., et al. (2007), Regional climate modeling for the developing world—The ICTP RegCM3 and RegCM3, *Bull. Am. Meteorol. Soc.*, *88*(9), 1395–1409.
- Peters, G. P., R. M. Andrew, T. Boden, J. G. Canadell, P. Ciais, C. Le Quééré, G. Marland, M. R. Raupach, and C. Wilson (2012), The challenge to keep global warming below 2°C, *Nat. Clim. Change*, *3*(1), 4–6.
- Piani, C., J. Haerter, and E. Coppola (2010), Statistical bias correction for daily precipitation in regional climate models over Europe, *Theor. Appl. Climatol.*, *99*(1–2), 187–192.
- Pielke, R. A., and R. L. Wilby (2012), Regional climate downscaling: What's the point?, *Eos Trans. AGU*, *93*(5), 52–53.
- Pierce, D. W., et al. (2013), The key role of heavy precipitation events in climate model disagreements of future annual precipitation changes in California, *J. Clim.*, *26*(16), 5879–5896.
- Quiroga, S., L. Garrote, A. Iglesias, Z. Fernández-Haddad, J. Schlickenrieder, B. de Lama, C. Mosso, and A. Sánchez-Arcilla (2011), The economic value of drought information for water management under climate change: A case study in the Ebro basin, *Nat. Hazards Earth Syst. Sci.*, *11*(3), 643–657.
- Radanovics, S., J.-P. Vidal, E. Sauquet, A. Ben Daoud, and G. Bontron (2013), Optimising predictor domains for spatially coherent precipitation downscaling, *Hydrol. Earth Syst. Sci.*, *17*(10), 4189–4208.
- Radu, R., M. Deque, and S. Somot (2008), Spectral nudging in a spectral regional climate model, *Tellus A*, *60*(5), 898–910.
- Rowell, D. (2011), Sources of uncertainty in future changes in local precipitation, *Clim. Dyn.*, *39*, 1929–1950.
- Ruiz-Ramos, M., A. Rodríguez, A. Dosio, C. Goodess, C. Harpham, M. Mínguez, and E. Sánchez (2016), Comparing correction methods of RCM outputs for improving crop impact projections in the Iberian Peninsula for 21st century, *Clim. Change*, *134*(1–2), 283–297.
- Rummukainen, M. (2010), State-of-the-art with regional climate models, *Wiley Interdiscip. Rev. Clim. Change*, *1*(1), 82–96.
- Samuelsson, P., C. G. Jones, U. Willén, A. Ullerstig, S. Gollvik, U. Hansson, C. Jansson, E. Kjellström, G. Nikulin, and K. Wyser (2011), The Rossby Centre regional climate model RCA3: Model description and performance, *Tellus A*, *63*(1), 4–23.
- Seneviratne, S. I., T. Corti, E. L. Davin, M. Hirschi, E. B. Jaeger, I. Lehner, B. Orlowsky, and A. J. Teuling (2010), Investigating soil moisture-climate interactions in a changing climate: A review, *Earth Sci. Rev.*, *99*(3–4), 125–161.
- Sumner, G., R. Romero, V. Homar, C. Ramis, S. Alonso, and E. Zorita (2003), An estimate of the effects of climate change on the rainfall of Mediterranean Spain by the late twenty first century, *Clim. Dyn.*, *20*(7–8), 789–805.
- Sunyer Pinya, M. A., et al. (2015), Inter-comparison of statistical downscaling methods for projection of extreme precipitation in Europe, *Hydrol. Earth Syst. Sci.*, *19*(4), 1827–1847.
- Taylor, K. E. (2001), Summarizing multiple aspects of model performance in a single diagram, *J. Geophys. Res.*, *106*(D7), 7183–7192.
- Teutschbein, C., and J. Seibert (2012), Bias correction of regional climate model simulations for hydrological climate-change impact studies: Review and evaluation of different methods, *J. Hydrol.*, *456–457*, 12–29.
- Teutschbein, C., and J. Seibert (2013), Is bias correction of regional climate model (RCM) simulations possible for non-stationary conditions?, *Hydrol. Earth Syst. Sci.*, *17*(12), 5061–5077.
- Themeßl, M. J., A. Gobiet, and G. Heinrich (2012), Empirical-statistical downscaling and error correction of regional climate models and its impact on the climate change signal, *Clim. Change*, *112*(2), 449–468, doi:10.1007/s10584-011-0224-4.
- Turco, M., and M. C. Llasat (2011), Trends in indices of daily precipitation extremes in Catalonia (NE Spain), 1951–2003, *Nat. Hazards Earth Syst. Sci.*, *11*(12), 3213–3226.
- Turco, M., P. Quintana-Seguí, M. C. Llasat, S. Herrera, and J. M. Gutiérrez (2011), Testing MOS precipitation downscaling for ensembles regional climate models over Spain, *J. Geophys. Res.*, *116*, D18109, doi:10.1029/2011JD016166.
- Turco, M., A. Sanna, S. Herrera, M.-C. Llasat, and J. M. Gutiérrez (2013), Large biases and inconsistent climate change signals in ENSEMBLES regional projections, *Clim. Change*, *120*(4), 859–869.
- Turco, M., M.-C. Llasat, J. von Hardenberg, and A. Provenzale (2014), Climate change impacts on wildfires in a Mediterranean environment, *Clim. Change*, *125*(3–4), 369–380.
- Uppala, S., et al. (2005), The ERA-40 re-analysis, *Q. J. R. Meteorol. Soc.*, *131*(612), 2961–3012.
- van der Linden, P., and J. Mitchell (Eds.) (2009), *ENSEMBLES: Climate Change and its Impacts: Summary of Research and Results from the ENSEMBLES Project*, 160 pp., Met Off. Hadley Cent, Exeter, U. K.
- Van Meijgaard, E., L. van Ulft, W. van de Berg, B. Bosveld, B. van der Hurk, G. Lenderik, and A. Siebesma (2008), The KNMI regional atmospheric climate model racmo version 2.1, *Tech. Rep. 302*, Royal Netherlands Meteorological Institute (KNMI), De Bilt, Netherlands. [Available at <https://www.rijksoverheid.nl/binaries/rijksoverheid/documenten/rapporten/2008/01/01/the-knmi-regional-atmospheric-climate-model-racmo-version-2-1/the-knmi-regional-atmospheric-climate-model-racmo-version-2-1.pdf>.]
- Walton, D. B., F. Sun, A. Hall, and S. Capps (2015), A hybrid dynamical–statistical downscaling technique. Part I: Development and validation of the technique, *J. Clim.*, *28*(12), 4597–4617.
- Wetterhall, F., F. Pappenberger, Y. He, J. Freer, and H. L. Cloke (2012), Conditioning model output statistics of regional climate model precipitation on circulation patterns, *Nonlinear Processes Geophys.*, *19*(6), 623–633.
- White, R. H., and R. Toumi (2013), The limitations of bias correcting regional climate model inputs, *Geophys. Res. Lett.*, *40*, 2907–2912, doi:10.1002/grl.50612.

World Meteorological Organization (2009), Guidelines on analysis of extremes in a changing climate in support of informed decisions for adaptation, *Tech. Rep. WCDMP No. 72 WMO/TD-No. 1500*, WMO, Geneva, Switzerland.

Zhang, X., L. Alexander, G. C. Hegerl, P. Jones, A. K. Tank, T. C. Peterson, B. Trewin, and F. W. Zwiers (2011), Indices for monitoring changes in extremes based on daily temperature and precipitation data, *Wiley Interdiscip. Rev. Clim. Change*, *2*(6), 851–870.

Zorita, E., J. Hughes, D. Lettemaier, and H. von Storch (1995), Stochastic characterization of regional circulation patterns for climate model diagnosis and estimation of local precipitation, *J. Clim.*, *8*(5), 1023–1042.